Inorganic Chemistry

Article

pubs.acs.org/IC

Synthesis, Electrochemistry, and Reactivity of Cerium(III/IV) Methylene-Bis-Phenolate Complexes

Brian D. Mahoney, Nicholas A. Piro, Patrick J. Carroll, and Eric J. Schelter*

P. Roy and Diana T. Vagelos Laboratories, Department of Chemistry, University of Pennsylvania, Philadelphia, Pennsylvania 19104, United States

Supporting Information

ABSTRACT: A series of cerium complexes containing a 2,2′-methylenebis(6-*tert*-butyl-4-methylphenolate) (MBP^{2-}) ligand framework is described. Electrochemical studies of the compound $[Li(THF)_2Ce(MBP)_2(THF)_2]$ (**1**) reveal that the metal based oxidation wave occurs at −0.93 V vs Fc/Fc^+. This potential demonstrates significant stabilization of the cerium(IV) ion in the MBP^{2-} framework with a shift of ∼2.25 V from the typically reported value for the cerium(III/IV) couple of $E^{\circ\prime}$ = +1.30 V vs Fc/Fc^+ for $Ce(ClO_4)_3$ in $HClO_4$ solutions. Compound **1** undergoes oxidation to form stable cerium(IV) species in the presence of a variety of common oxidants. The coordination of the redox-active ligands 2,2′-bipyridine and benzophenone to **1** result in complexes in which no apparent metal-to-ligand charge transfer occurs and the cerium ion remains in the +3 oxidation state.

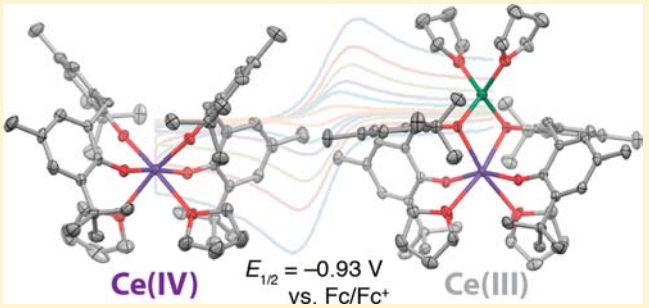

INTRODUCTION

One-electron redox chemistry is an important aspect of the chemistry of the lanthanides.[1−3] Divalent samarium reagents such as samarium diiodide have found widespread use as potent, general one-electron reductants, while ceric ammonium nitrate and related complexes are of interest due to their application as oxidants.[4,5] Whereas the reductive chemistry of the lanthanides has advanced considerably in recent years,[6−9] the oxidative chemistry of cerium has seen relatively less development.[10−13] The unique oxidative utility of cerium compared with other lanthanides results from the relative accessibility of its $4f^0$ tetravalent oxidation state. Due to a large formal oxidation potential, $E^{\circ\prime}$ = +1.30 V vs Fc/Fc^+ for $Ce(ClO_4)_3$ in $HClO_4$ solutions,[14] cerium(IV) reagents are commonly applied in chemical transformations as strong oxidants. However, the cerium(III/IV) redox couple is highly sensitive to conditions and ligand environments.

At high pH, aqueous solutions of cerium(III) carbonates are spontaneously oxidized by O_2 to form a cerium(IV)−peroxo complex.[15] Nonaqueous electrochemical studies of cerium complexes have reported formal reversible cerium(III/IV) couples shifted as far as −1.40 V vs Fc/Fc^+.[16−18] However, the ability to use cerium(III) as a reductant in organic chemical transformations has yet to be demonstrated. We recently reported the electrochemistry of $[Li_3(THF)_4(BINOLate)_3Ce^{III}(THF)]$, which shows a quasi-reversible oxidation with E_{pa} = −0.45 V vs Fc/Fc^+ in THF.[19] The favorable thermodynamics for electron transfer from $[Li_3(THF)_4(BINOLate)_3Ce^{III}(THF)]$ suggest the possibility of applying cerium(III) complexes as reducing agents. The replacement of samarium(II) reagents with cerium(III) compounds is of interest due to the large abundance of cerium in the earth's crust and its low cost. Cerium is inexpensive due to its occurrence as a major byproduct in the separation of light rare earths from bastnaesite and monazite ores.[20] An understanding of cerium(III) electrochemistry and the chemical oxidation of cerium(III) complexes is crucial to developing the utility of cerium(III) as a reductant.[10,16−18,21−28]

Despite some progress in this area, straightforward one-electron oxidation reactions to produce cerium(IV) products remain nontrivial.[12] It has been established that electron-deficient tetravalent cerium ions are most effectively supported by strongly electron donating ligands.[10,18,22,26−28] Our work on the $[M_3(THF)_x(BINOLate)_3Ce^{III}(THF)_y]$ (M = Li, Na, K) system highlighted the importance of ligand reorganization in such chemical oxidation reactions of cerium(III). We reasoned that cerium complexes of methylene-bis-phenolate ligands (H_2MBP, Figure 1) bearing a heterobimetallic Li−Ce−MBP framework would similarly mitigate the ligand reorganization component of the oxidation reaction and provide facile access to cerium(IV) congeners. In addition, the presence of both −^{t}Bu and −Me substituents on the MBP^{2-} framework provide

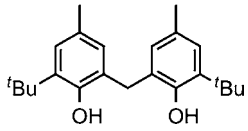

Figure 1. 2,2′-Methylenebis(6-*tert*-butyl-4-methylphenol) (H_2MBP).

Received: January 26, 2013
Published: April 26, 2013

   dx.doi.org/10.1021/ic400202r | *Inorg. Chem.* 2013, 52, 5970−5977

Scheme 1. Synthesis and Reactivity of Ce−MBP Complexes

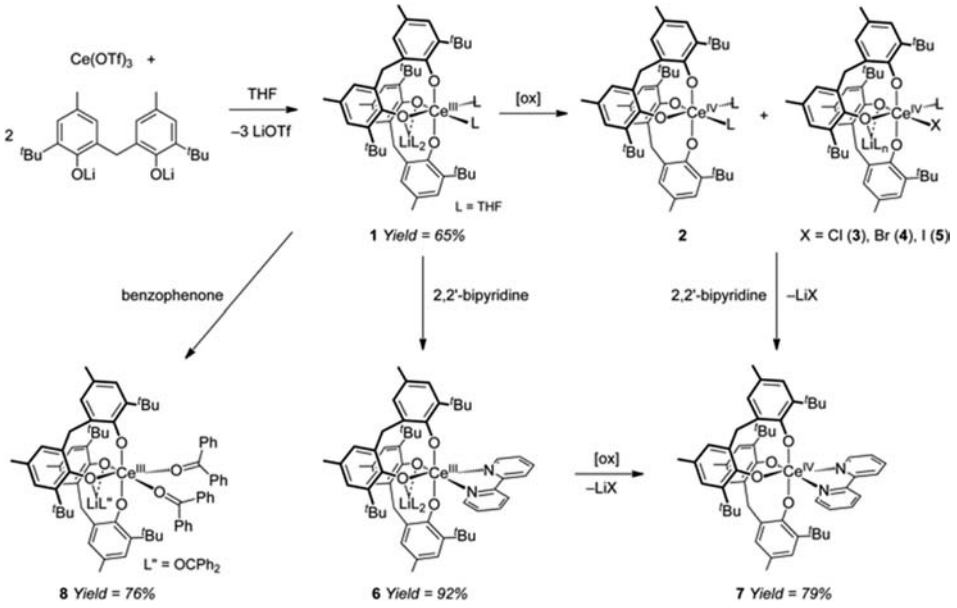

for an electron-rich aryloxide ligand that is conducive to supporting the electron-deficient cerium(IV) ion. Finally, the steric demands of the $-^{t}$Bu group contribute to maintaining open coordination sites at the lanthanide ion, which has also been implicated as a requirement for straightforward isolation of cerium(IV) complexes.[19] In this context, we sought to prepare cerium(III) complexes of the MBP^{2-} ligand and to explore their electrochemical properties and chemical oxidation.

RESULTS AND DISCUSSION

Rare earth and thorium complexes of the 2,2′-methylenebis(6-*tert*-butyl-4-methylphenolate) (MBP^{2-}) ligand framework have been reported,[29−34] but the related cerium complexes are unreported to this point. Reaction of $Ce(OTf)_3$ with 2 equiv of $Li_2MBP(THF)_3$ in THF at room temperature afforded $[Li(THF)_2Ce^{III}(MBP)_2(THF)_2]$ (**1**) in good yield (Scheme 1). ^{1}H NMR spectroscopy on the product mixture indicated the formation of a paramagnetic compound with broadened and shifted ^{1}H resonances that ranged from −4.36 to +13.99 ppm in C_5D_5N. The four ligand resonances indicated the complex is C_2 symmetric in solution and the peaks were assigned based on integration. ^{7}Li NMR spectroscopy indicated a single peak that was broadened and shifted to +4.36 ppm. Compound **1** is air-sensitive, with exposure of solutions of **1** to atmosphere leading to an intractable mixture of dark purple products with diamagnetic ^{1}H resonances. Characterization of **1** by single-crystal X-ray diffraction revealed Ce−OAr bonds that ranged from 2.3146(10)−2.3693(10) Å (Figure 2). The bond distances agreed with the reported isostructural complex $[Na(THF)_2Nd(MBP)_2(THF)_2]$ when accounting for the 0.027 Å difference in size between the metal ions.[35] The Nd−OAr bonds in $[Na(THF)_2Nd(MBP)_2(THF)_2]$ ranged from 2.278(2)−2.315(2) Å.[31,35]

Electrochemical characterization of **1** in THF solution revealed a reversible oxidation wave centered at $E_{1/2}$ = −0.93 V versus Fc/Fc^+ (Figure 3). The electron-rich MBP^{2-} ligand field decreases the reduction potential of the cerium(III/IV) couple by ∼2.25 V relative to the standard reported oxidation potential for cerium(III).[36] This shift of potential places

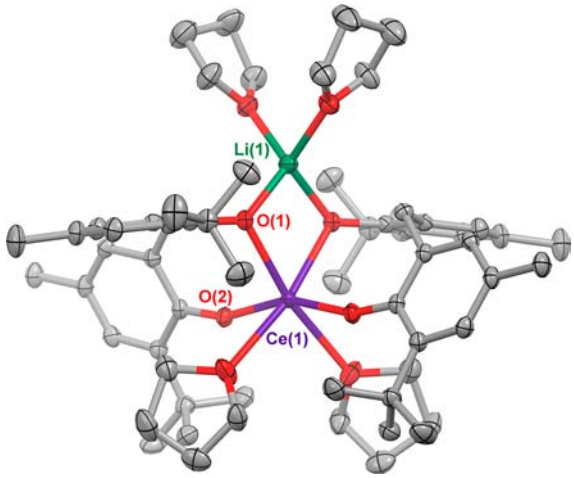

Figure 2. Thermal ellipsoid plot of $[Li(THF)_2Ce(MBP)_2(THF)_2]$ (**1**) at the 50% probability level. Hydrogen atoms have been omitted for clarity. Selected bond distances (Å): Ce−O(1) 2.3693(10); Ce−O(2) 2.3146(10).

complex **1** among the most reducing cerium(III) compounds reported and indicates strong stabilization of the formal cerium(IV) ion by the MBP^{2-} ligand framework. It is noteworthy that complex **1** is a more potent reductant than the Eu(II) ion, as the standard potential for Eu(II) is $E^{\circ\prime}$ = −0.75 vs Fc/Fc^+.[6] This is also noteworthy given that $Eu(C_5Me_5)_2$ is known to undergo one-electron transfer to certain α-diimines upon coordination.[37−39] Having established that the metal-based oxidation of **1** is favored thermodynamically, we set out to explore the chemical oxidation of the complex.

Stirring solutions of **1** in THF or toluene over $CuCl_2$ resulted in an immediate color change to a dark purple solution that exhibited sharp ^{1}H NMR resonances ranging from +1.36 to +7.36 ppm, consistent with the formation of a closed-shell complex. The oxidant byproduct was removed by filtration, and the cerium products were crystallized by layering a concentrated THF solution with pentane. This resulted in

dx.doi.org/10.1021/ic400202r | Inorg. Chem. 2013, 52, 5970−5977

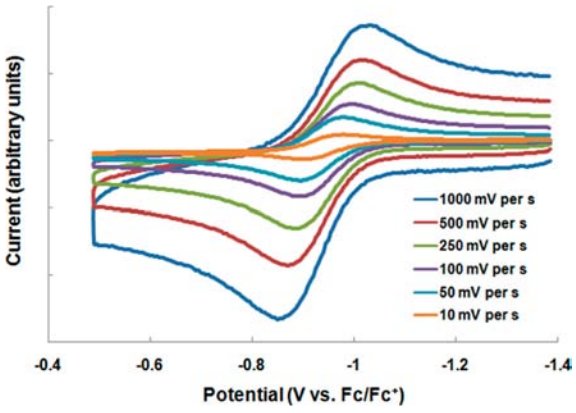

Figure 3. Cyclic voltammograms of compound **1** displaying the scan rate dependence of the cerium(III) oxidation and return reduction in THF. Potentials are referenced to a Fc/Fc^+ internal standard with 100 mM $[^nPr_4N][BAr^F{}_4]$ supporting electrolyte and ~1 mM analyte concentration.

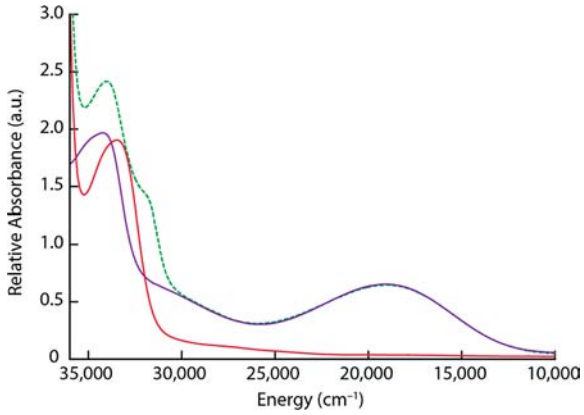

Figure 4. Electronic absorption spectra showing a ligand-π to Ce-4f charge transfer absorption for the Ce^{IV} complex **2** (purple trace) in the visible range (E_{max} = 19 050 cm^{-1}; λ_{max} = 525 nm, ε = ~4800 M^{-1} cm^{-1}) in comparison with complex **1** (red trace) and complex **7** (green dashed trace).

cocrystallization of $Ce(MBP)_2(THF)_2$ (**2**) and the −ate complex $[Li(THF)_3CeCl(MBP)_2(THF)]$ (**3**) in ~4:1 ratio. The product distribution was approximated using ^1H NMR spectroscopy on the isolated crystals. Analogous reactions with $CuBr_2$ or I_2 as the oxidants afforded mixtures of **2** and $[Li(THF)_3CeBr(MBP)_2(THF)]$ (**4**) or $[Li(THF)CeI(MBP)_2(THF)]$ (**5**), respectively. Similar mixtures of products were obtained by reaction with the copper(I) reagents CuX (X = Cl, Br, I) in toluene, though these reactions proceed more slowly. On exposure to atmosphere compounds **2**−**5** decompose over the course of days due to protonation of the MBP^{2-} ligand by moisture, as evident by the appearance of H_2MBP in the NMR spectra of the products.

The competition between LiX salt elimination to form $Ce(MBP)_2(THF)_2$ (**2**) and −ate complex formation to form **3**, **4**, or **5** was found to be influenced by reaction solvent and crystallization conditions. However, dissolving the mixtures of solids in either coordinating or noncoordinating solvents, followed by filtration and crystallization, did not lead to straightforward purification of the products. Crystallization at either room temperature or −30 °C similarly resulted in cocrystallization of the product mixture in varying ratios. Thus, in our hands a reliable route to isolate either **2** or **3**−**5** independent of the other could not be determined. Oxidation reactions of **1** using *N*-bromosuccinimide, $[Fc][PF_6]$, and Ph_3CCl also produced mixtures and attempts to crystallize single products from these reactions were similarly unsuccessful.

On an occasion where a small amount of relatively pure crystalline **2** was isolated, it was characterized by UV−vis spectroscopy, Figure 4. The spectrum of **2** reveals a broad band at ~19 000 cm^{-1} that corresponds to a ligand-π to vacant Ce-4f transition, which is the electronic transition underlying the compound's dark purple color. A broad, intense transition such as this is characteristic of Ce(IV) complexes.[40,41] The spectrum of the colorless complex **1** is shown for comparison and displays only transitions in the UV region associated with ligand-centered transitions; the Ce(III) f−f transition is typically very low in energy (<3000 cm^{-1}) and hence not observed in our experimental spectral range.[42]

Despite the difficulties in obtaining analytically pure cerium(IV) complexes by direct oxidation of **1**, it was possible to obtain X-ray structural information on crystals of **2**−**5**. Diffraction studies on compounds **2**−**5** revealed that the products were similarly six-coordinate cerium ions (Figure 5). The Ce−OAr bond lengths in **2**−**5** shorten to 2.113(2)−2.204(3) Å, in accordance with the decrease in the cerium(III/IV) ionic radius from 1.01 to 0.87 Å.[35] For complex **2**, the two THF ligands are retained at the cerium(IV) ion in *cis*-coordination sites following oxidation. Complex **3** exhibits a chloride ion loosely coordinated to the cerium(IV) ion with a Ce^{IV}−Cl distance of 2.7641(8) Å. A four-coordinate lithium cation is also associated with the cerium-bound chloride ligand with a Li−Cl −ate complex interaction of 2.337(6) Å. Three THF molecules complete the coordination sphere of the tetrahedral lithium cation. Electrochemical studies on mixtures of **2** and **3** show a reversible reduction occurring at the same potential as the oxidation of **1** (Figure S1, Supporting Information).

In order to improve the conversion to an isolable cerium(IV) product, 2,2′-bipyridine (bpy) was used as a chelating ligand for the cerium ion to promote elimination of the LiX salt. Reaction of **1** with 2,2′-bipyridine and subsequent crystallization from THF/hexane led to isolation of $[Li(THF)_2Ce(MBP)_2(bpy)]$ (**6**) in good yield. Structural determination of **6** revealed a six-coordinate Ce^{III} ion where the bpy ligand fits into the cleft formed by the two MBP^{2-} ligands (Figure 6). Two independently refined complexes are present in the asymmetric unit of this complex. The Ce−N_{bpy} bond distances were unsymmetric between the two Ce−N_{bpy} sites with Ce−N(1) 2.684(6) or 2.680(6) Å and Ce−N(2) 2.748(6) or 2.747(6) Å. The Ce−O bond distances ranged from 2.208(5) to 2.415(6) Å, with the longer Ce−O bond lengths due to coordination of the Li cation to two of the oxygen atoms. Oxidation of **6** by CuX_2 (X = Cl^- or Br^-) in THF solutions produced a single product, which was assigned as $Ce(MBP)_2(bpy)$ (**7**) based upon ^1H and ^7Li NMR spectroscopy and subsequently confirmed by elemental analysis. Complex **7** could also be obtained by reactions of **2**−**5** with 2,2′-bipyridine, as verified by NMR spectroscopy (Scheme 1). The electronic absorption spectrum of **7** shows the same low-energy charge transfer band as observed for **2**, in addition to increased UV absorbance that is assigned to transitions within the bipyridine ligand (Figure 4).

In addition to providing an isolable cerium(IV) complex of this system, the isolation of the bpy complexes **6** and **7**

dx.doi.org/10.1021/ic400202r | Inorg. Chem. 2013, 52, 5970−5977

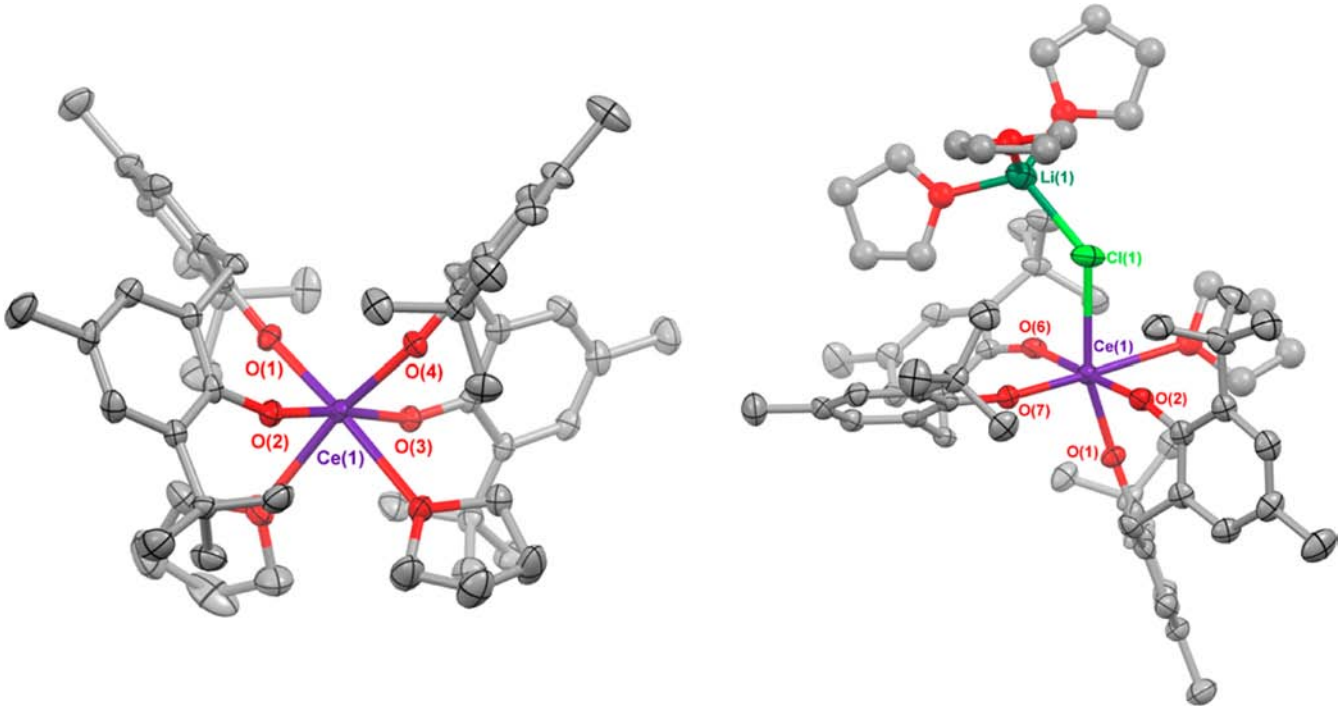

Figure 5. Thermal ellipsoid plots of $Ce(MBP)_2(THF)_2$ (**2**, left) and $[Li(THF)_3CeCl(MBP)_2(THF)]$ (**3**, right) at the 50% probability level. Hydrogen atoms and interstitial solvent molecules have been omitted for clarity. Selected bond distances (Å): (**2**) Ce–O(1) 2.124(2), Ce–O(2) 2.152(2), Ce–O(3) 2.145(2), Ce–O(4) 2.113(2); (**3**) Ce–O(1) 2.1376(18), Ce–O(2) 2.1540(18), Ce–O(6) 2.1602(17), Ce–O(7) 2.1265(18), Ce–Cl 2.7641(8).

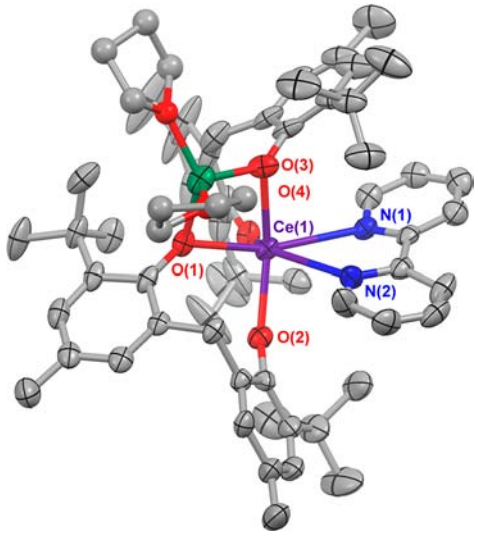

Figure 6. Thermal ellipsoid plot for one independent molecule of $[Li(THF)_2Ce(MBP)_2(bpy)]$ (**6**) at the 50% probability level. Hydrogen atoms, the second independent molecule, and interstitial solvents have been omitted for clarity. Selected bond distances (Å): Ce–O(1) 2.390(5), 2.421(5); Ce–O(2) 2.258(6), 2.208(5); Ce–O(3) 2.415(6), 2.408(6); Ce–O(4) 2.258(5), 2.236(5); Ce–N(1) 2.684(6), 2.680(6); Ce–N(2) 2.748(6), 2.747(6).

warranted investigation of their electronic structures. The use of 2,2′-bipyridine as a ligand allowed the incorporation of a redox-active group with the potential to act as an electron acceptor. In reported lanthanide and actinide chemistry, coordination of an electron-accepting redox-active ligand has resulted in charge-separated compounds that exhibit unique electronic structure properties and reactivity.[43,44] In our hands, the first reduction wave of 2,2′-bipyridine in THF was measured at $E_{1/2}$ = −2.60 V vs Fc/Fc^+. This potential is 1.67 V more reducing than the observed oxidation of **1** at $E_{1/2}$ = −0.93 V versus Fc/Fc^+. However coordination of terpyridine to lanthanide cations is known to shift its reduction potential by up to +0.94 V,[45] while coordination of carbonyls can lead to shifts of up to +1.3 V.[46] These results suggested that the reduction of 2,2′-bipyridine by **1** could be thermodynamically feasible upon coordination despite the large difference in formal potential between the constituent metal oxidation and ligand reduction potentials. These observations prompted us to evaluate possible metal–ligand charge separation in complex **6**.

The solution electrochemistry of **6** measured in THF shows the cerium(III) oxidation and 2,2′-bipyridine reduction processes are unchanged compared with the measurement of those constituents alone under the same conditions (Figure S3, Supporting Information).[47] This is in agreement with the observation that the cerium complex and 2,2′-bipyridine are not associated in THF solutions based on ^{1}H NMR and electronic absorption spectroscopy. Thus solution studies of **6** dissolved in THF demonstrated that the bipyridine ligand is displaced by THF in solution, and we therefore relied on assignment of the electronic structure based on solid-state characterization.

To determine the electronic structure of **6** in the solid state, the redox inactive lanthanum analogue, $[Li(THF)_2La(MBP)_2(bpy)]$ (**6-La**), was synthesized. The electronic structure of this compound is unambiguous because metal-to-ligand charge transfer cannot occur from the $4f^05d^0$ lanthanum(III) cation. A comparison of the bond metrics based on X-ray diffraction showed no significant differences between **6** and **6-La** within the 2,2′-bipyridine ligand (Table 1).[48,49] Comparisons with representative lanthanide–bpy adducts from the literature demonstrate that the bipyridine bond lengths are in

dx.doi.org/10.1021/ic400202r | Inorg. Chem. 2013, 52, 5970–5977

Table 1. Comparison of 2,2′-Bipyridine Bond Lengths of $[Li(THF)_2La(MBP)_2(bpy)]$ (6-La), $[Li(THF)_2Ce(MBP)_2(bpy)]$ (6), $La(NO_3)_3(bpy)_2$,[48,49] and $Sm^{III}(Cp^*)_2(bpy)^{\bullet-}$[48,49]

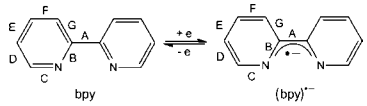

	A	B	C	D	E	F	G
$[Li(THF)_2La(MBP)_2(bpy)]$	1.484(10)	1.315(9)	1.319(9)	1.357(10)	1.343(12)	1.335(13)	1.369(9)
	1.512(10)	1.344(8)	1.325(10)	1.374(10)	1.355(12)	1.354(12)	1.394(9)
		1.346(8)	1.331(10)	1.381(10)	1.361(13)	1.385(12)	1.397(9)
		1.372(9)	1.372(10)	1.387(11)	1.392(12)	1.416(13)	1.399(9)
		1.304(11)	1.324(12)	1.348(12)	1.334(14)	1.331(15)	1.374(12)
$[Li(THF)_2Ce(MBP)_2(bpy)]$	1.476(12)	1.341(10)	1.327(12)	1.369(12)	1.340(15)	1.345(15)	1.386(11)
	1.520(11)	1.343(10)	1.332(12)	1.379(12)	1.360(15)	1.388(14)	1.394(12)
		1.369(11)	1.379(12)	1.390(13)	1.412(15)	1.420(15)	1.404(10)
$La(NO_3)_3(bpy)_2$	1.450(17)	1.326(15)	1.328(16)	1.426 (20)	1.395 (24)	1.392(23)	1.405(20)
		1.363 (16)	1.340 (20)	1.409 (20)	1.411 (21)	1.394 (22)	1.412(17)
$Sm^{III}(Cp^*)_2(bpy)^{\bullet-}$	1.429(4)	1.378(4)	1.353(4)	1.365 (5)	1.397(7)	1.335(7)	1.416(4)
		1.388(4)	1.359(4)	1.372(5)	1.414(7)	1.339(6)	1.421(4)

close agreement with compounds bearing a neutral coordinated 2,2′-bipyridine. On the basis of this data, we assigned the electronic structure of **6** as cerium(III)−(2,2′-bipyridine)^0.

To further explore the possibility of synthesizing charge-separated cerium complexes, the reactivity of **1** with benzophenone, Ph_2CO, was explored. A recent report of coordination of Ph_2CO to $Ce[N(TMS)_2]_3$ and $Ce(C_5H_5)_3$ found that in both cases cerium to ligand charge transfer does not occur.[46] However, the electrochemistry of **1** demonstrates that the cerium(III/IV) couple in the MBP^{2-} framework occurs at substantially more reducing potentials than in the silylamide or cyclopentadienide ligand frameworks.[19,50] The reduction potential of Ph_2CO was measured at −2.31 V vs Fc/Fc^+ in THF, demonstrating that it is easier to reduce than 2,2′-bipyridine. The addition of Ph_2CO to **1** in toluene results in a color change from colorless to red. The product was crystallized in the presence of 3 equiv of Ph_2CO to produce $[Li(Ph_2CO)Ce(MBP)_2(Ph_2CO)_2]$ (**8**) in good yield (Figure 7). Infrared spectroscopy shows carbonyl stretching frequencies of 1629 and 1619 cm^{-1} for **8** compared with 1654 cm^{-1} for free benzophenone. This shift in stretching frequency is consistent with coordination to a Lewis acid rather than reduction of the benzophenone with reported examples of coordinated, reduced benzophenone showing a shift of the carbonyl stretch of ∼100 cm^{-1}.[51] Additionally, the C═O bond distances in **8** ranged from 1.230(3) to 1.236(4) Å compared with 1.223(2) Å for free benzophenone,[52] while reduction of Ph_2CO coordinated to a lanthanide typically results in a lengthening of this bond by over 0.1 Å.[53] As such, we assign the electronic structure of the benzophenone complex **8** as Ce^{III}−(benzophenone)$_3^0$. Based on these results, it is evident that more easily reduced electron-accepting groups or more strongly electron-donating supporting ligands are required to isolate charge-separated cerium complexes and to develop the potential use of cerium(III) as a one-electron reductant.

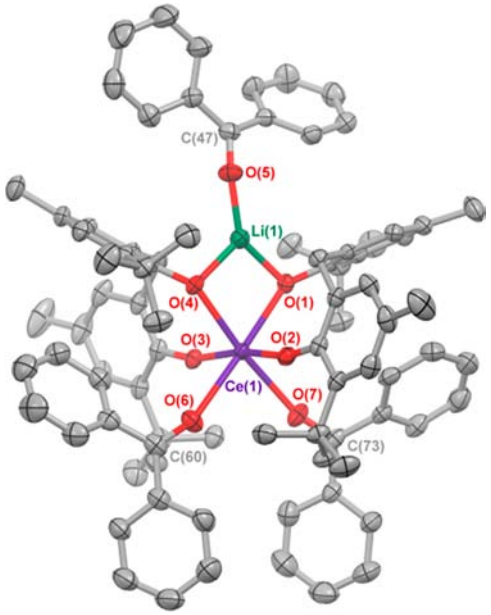

Figure 7. Thermal ellipsoid plot of $[Li(Ph_2CO)Ce(MBP)_2(Ph_2CO)_2]$ (**8**) at the 50% probability level. Hydrogen atoms and interstitial solvents have been omitted for clarity. Selected bond distances (Å): Ce−O(1) 2.3316(19), Ce−O(2) 2.2714(18), Ce−O(3) 2.2800(18), Ce−O(4) 2.3371(18), Ce−O(6) 2.530(2), Ce−O(7) 2.513(2), O(5)−C(47) 1.230(3), O(6)−C(60) 1.236(4), O(7)−C(73) 1.233(3).

CONCLUSIONS

The coordination of electron-rich MBP^{2-} donors and the use of nonaqueous conditions served to reduce the reduction potential of the cerium(III/IV) couple by ∼2.25 V versus the standard reported potential for aqueous cerium(III) and provided an isolable cerium(III) compound that is best classified thermodynamically as a mild reductant.[36] In the isolation of cerium(IV)−MBP complexes, the products of one-electron oxidation reactions were dependent upon the competition between salt elimination and −ate complex formation. The resulting cerium(IV) compounds were stable toward O_2. We reported rare electrochemical data for the cerium(III/IV) couple in a nonaqueous system. The coordination of 2,2′-bipyridine and Ph_2CO as redox-active electron acceptors did not induce electron transfer from the metal center. Efforts are currently underway to develop more electron-donating ligand frameworks that provide more strongly reducing cerium(III) compounds as well as to

dx.doi.org/10.1021/ic400202r | Inorg. Chem. 2013, 52, 5970−5977

incorporate substrates with more accessible redox couples into the Ce−MBP framework.

EXPERIMENTAL SECTION

General Considerations. Unless otherwise indicated all reactions and manipulations were performed under an inert atmosphere (N_2) using standard Schlenk techniques or in a Vacuum Atmospheres, Inc., Nexus II drybox equipped with a molecular sieves 13X/Q5 Cu-0226S catalyst purifier system. Glassware was oven-dried overnight at 150 °C prior to use. ^{1}H NMR spectra were obtained on a Bruker DMX-300 or on a Bruker AM-500 Fourier transform NMR spectrometer at 300 or 400 MHz, respectively. ^{7}Li{^{1}H}-NMR were recorded on a Bruker AM-500 Fourier transform NMR spectrometer at 194 MHz. Proton chemical shifts were recorded in units of parts per million downfield from TMS by referencing to residual proteo solvent peaks. The ^{7}Li{^{1}H} spectra were referenced to external solution standards of LiCl in H_2O (at zero ppm). Elemental analyses were performed at the University of California, Berkeley, Microanalytical Facility using a Perkin-Elmer series II 2400 CHNS analyzer. Solution UV−vis/near-IR spectra were collected on a PerkinElmer Lambda 950 UV/vis/NIR spectrometer at concentrations of 0.1 to 5 mM. One millimeter path length screw cap quartz cells were used with a blank measured before each run. The infrared spectra were obtained from 400 to 4000 cm^{-1} using a Perkin-Elmer 1600 series infrared spectrometer.

Electrochemistry. Voltammetry experiments were performed using a CH Instruments 620D electrochemical analyzer/workstation, and the data were processed using CHI software v 9.24. All experiments were performed in a N_2 atmosphere drybox using electrochemical cells that consisted of a 4 mL vial, glassy carbon (3 mm diameter) working electrode, a platinum wire counter electrode, and a silver wire plated with AgCl as a quasi-reference electrode. The working electrode surfaces were polished prior to each set of experiments and were periodically replaced to prevent the buildup of oxidized or reduced products on the electrode surfaces. Solutions employed during CV studies were ∼1 mM in analyte and 100 mM in [^{n}Pr$_4$N][B(3,5-(CF$_3$)$_2$-C$_6$H$_3$)$_4$]. Potentials were reported versus Fc/Fc$^+$, which was added as an internal standard for calibration at the end of each run. All data were collected in a positive-feedback IR compensation mode to minimize uncompensated resistance in the solution cells. The THF solution cell resistances were measured prior to each run to ensure resistances ∼1500 Ω or less.

Materials. Tetrahydrofuran, diethyl ether, dichloromethane, fluorobenzene, hexanes, and pentane were purchased from Fisher Scientific. The solvents were sparged for 20 min with dry N_2 and dried using a commercial two-column solvent purification system comprising columns packed with Q5 reactant and neutral alumina (for hexanes and pentane) or two columns of neutral alumina (for THF, Et_2O, and toluene). Deuterated solvents were purchased from Cambridge Isotope Laboratories, Inc., and stored over potassium mirror overnight prior to use. Cerium(III) triflate (Strem Chemicals Inc.) was heated at 150 °C for 12 h at ∼100 mTorr prior to use. 2,2′-Bipyridine was purchased from Acros Organics and purified by sublimation prior to use. 2,2′-Methylenebis(6-*tert*-butyl-4-methylphenolate) was purchased from Sigma Aldrich and used without further purification. Li[N(TMS)$_2$] was purchased from Acros Organics and recrystallized from toluene prior to use. The supporting electrolyte, [^{n}Pr$_4$N][B(3,5-(CF3)$_2$-C$_6$H$_3$)$_4$] ([^{n}Pr$_4$N][BAr$^F{}_4$]), was prepared according to literature procedures.[54]

X-ray Crystallography. X-ray reflection intensity data were collected on a Bruker APEXII CCD area detector employing graphite-monochromated Mo Kα radiation (λ = 0.71073 Å) at a temperature of 143(1) K. In all cases, rotation frames were integrated using SAINT,[55] producing a listing of unaveraged F^2 and $\sigma(F^2)$ values, which were then passed to the SHELXTL[56] program package for further processing and structure solution. The intensity data were corrected for Lorentz and polarization effects and for absorption using TWINABS[57] or SADABS.[58] The structures were solved by direct methods (SHELXS-97) and refinement was by full-matrix least-squares based on F^2 using SHELXL-97.[59] All reflections were used during refinements. The weighting scheme used was $w = 1/[\sigma^2(F_o^2) + (aP)^2 + bP]$ where $P = (F_o^2 + 2F_c^2)/3$ and a and b are refined. Non-hydrogen atoms were refined anisotropically, and hydrogen atoms were refined using a riding model. In the cases where difference Fourier peaks suggested that disordered solvent was present in the lattice but for which a reliable model could not be built, the data were treated using PLATON-SQUEEZE.[60]

Li$_2$MBP(THF)$_3$. A 20 mL scintillation vial was charged with H_2MBP (1.98 g, 5.82 mmol) dissolved in 15 mL of THF. Solid Li[N(TMS)$_2$] (2.16 g, 12.90 mmol, 2.2 equiv) was added, causing a color change to dark green-brown. After 3 h, the solution had turned tan, and the product precipitated as a white solid. The reaction mixture was dried under reduced pressure, and the product was washed with pentane and collected (2.84 g, 4.99 mmol, 86%). ^{1}H NMR (C$_6$D$_6$, 400 MHz, 298 K): δ 7.40 (s, 2H, Ar*H*), 7.15 (s, 2H, Ar*H*), 4.22 (bs, 2H, C*H*$_2$), 3.31 (t, 12H, C$_4$*H*$_8$O), 2.31 (s, 6H, C*H*$_3$), 1.58 (s, 18H, C(C*H*$_3$)$_3$), 1.27 (t, 12H, C$_4$*H*$_8$O).

[Li(THF)$_2$Ce(MBP)$_2$(THF)$_2$] (1). A 20 mL scintillation vial was charged with Li$_2$MBP(THF)$_3$ (1.65 g, 2.91 mmol) dissolved in 15 mL of THF, and Ce(OTf)$_3$ (0.81 g, 1.38 mmol) was added. After 3 h, all of the solids had dissolved to produce a pale orange solution. The reaction mixture was stripped of volatiles under reduced pressure, and the residue was suspended in 60 mL of toluene. The toluene solution was filtered through a Celite-packed coarse porosity fritted filter, and the volatiles were removed to produce a white residue. The white solid was washed with cold pentane, dissolved in 8 mL of THF, and filtered through a Celite-packed Pasteur pipet. Crystalline colorless solids suitable for X-ray crystallography and elemental analysis were grown overnight by layering the concentrated THF solution with 20 mL of pentane (999 mg, 0.89 mmol, 65%). ^{1}H NMR (C$_5$D$_5$N, 300 MHz, 298 K): δ 13.99 (bs $\Delta\nu_{1/2}$ = 20 Hz, 4H, Ar*H*$_2$), 9.75 (bs $\Delta\nu_{1/2}$ = 25 Hz, 4H Ar*H*), 5.03 (s $\Delta\nu_{1/2}$ = 7 Hz, 12H, C*H*$_3$), 3.63 (m, 16H, C$_4$*H*$_8$O), 1.60 (m, 16H, C$_4$*H*$_8$O), −4.36 (bs $\Delta\nu_{1/2}$ = 90 Hz, 18H, C(C*H*$_3$)$_3$). ^{7}Li NMR (C$_5$D$_5$N, 400 MHz, 298 K): δ 4.36. Anal. Calcd for C$_{62}$H$_{92}$CeLiO$_8$: C, 66.94; H, 8.34. Found: C, 66.57; H, 8.17.

General Procedure for the Oxidations of 1 To Form Compounds 2−5. To a solution of **1** (0.86 g, 0.76 mmol) in 10 mL of toluene was added 1 equiv of $CuCl_2$, $CuBr_2$, or I_2, causing an immediate color change to dark purple. After 1 h, the solution was filtered through a Celite-packed Pasteur pipet and stripped of volatiles under reduced pressure. The solids were dissolved in 4 mL of THF, and the solution was filtered through a Celite-packed Pasteur pipet and layered with 15 mL of pentane. Crystals were grown over 7 days at −30 °C and were found to contain mixtures of **2** with **3**, **4**, or **5** by ^{1}H NMR spectroscopy.

[Li(THF)$_2$Ce(MBP)$_2$(bpy)] (6). A 20 mL scintillation vial was charged with **1** (619 mg, 0.556 mmol) dissolved in 10 mL of toluene. Solid 2,2′-bipyridine (89 mg, 0.57 mmol) was added, causing an immediate color change to dark red. After 2 h, the cloudy orange solution was stripped of volatiles under reduced pressure. The orange solid residue was dissolved in 3 mL of THF then filtered through a Celite-packed Pasteur pipet. Dark red crystalline solids suitable for X-ray crystallography and elemental analysis were grown over 48 h by layering of the concentrated THF solution with 15 mL of hexane (575 mg, 0.511 mmol, 92%). ^{1}H NMR (C$_5$D$_5$N, 400 MHz, 298 K): δ 14.11 (bs, 4H, Ar*H*$_2$), 9.80 (bs, 4H Ar*H*$_2$), 8.69 (t, 2H, py-*H*), 7.74 (t, 2H, bpy-*H*), 5.08 (s, 12H, C*H*$_3$), 3.65 (s, 8H, C$_4$*H*$_8$O), 1.61 (s, 8H, C$_4$*H*$_8$O), −4.44 (bs, 36H, C(C*H*$_3$)$_3$). ^{7}Li NMR (C$_5$D$_5$N, 400 MHz, 298 K): δ 2.88 (s). Anal. Calcd for C$_{64}$H$_{84}$CeLiN$_2$O$_6$: C, 68.36; H, 7.53; N, 2.49. Found: C, 68.16; H, 7.80; N, 2.32.

[Li(THF)$_2$La(MBP)$_2$(THF)$_2$]. The lanthanum analog of **1** was prepared by analogous reaction of La(OTf)$_3$ with Li$_2$MBP to afford [Li(THF)$_2$La(MBP)$_2$(THF)$_2$] (287 mg, 0.258 mmol, 51%). ^{1}H NMR (C$_5$D$_5$N, 400 MHz, 298 K): δ 7.54 (d, J = 1.6 Hz, 4H, Ar*H*$_2$), 7.10 (d, J = 2.0 Hz, 4H, Ar*H*$_2$), 5.56 (d, J = 13.2 Hz, 2H, C*H*$_2$), 3.76 (d, J = 13.2 Hz, 2H, C*H*$_2$), 3.67 (m, 12 H, C$_4$*H*$_8$O), 2.33 (s, 12H, C*H*$_3$), 1.63 (m, 12 H, C$_4$*H*$_8$O), 1.53 (s, 36H, C(C*H*$_3$)$_3$) ^{7}Li NMR (C$_5$D$_5$N, 400 MHz, 298 K): δ 4.64 (s). Anal. Calcd for C$_{62}$H$_{92}$LaLiO$_8$: C, 67.01; H, 8.34. Found: C, 66.91; H, 8.16.

dx.doi.org/10.1021/ic400202r | Inorg. Chem. 2013, 52, 5970−5977

[Li(THF)$_2$La(MBP)$_2$(bpy)] (6-La). Compound **6-La** was prepared by reaction of [Li(THF)$_2$La(MBP)$_2$(THF)$_2$] with 2,2′-bipyridine under identical conditions used for the synthesis of **6** (67 mg, 0.060 mmol, 69%). ^{1}H NMR (C_5D_5N, 400 MHz, 298 K): δ7.54 (d, 4H, ArH_2), 7.10 (d, 4H, ArH_2), 5.55 (d, 2H, CH_2), 3.76 (d, 2H, CH_2), 3.67 (s, 8H, C_4H_8O), 2.33 (s, 12H, CH_3), 1.63 (s, 8H, C_4H_8O), 1.53 (s, 36H, C(CH_3)) ^{7}Li NMR: δ 4.64 (s). Anal. Calcd for $C_{64}H_{84}LaLiN_2O_6$: C, 68.44; H, 7.54; N, 2.49. Found: C, 68.34; H, 7.60; N, 2.28.

Ce(MBP)$_2$(bpy) (7). A 20 mL scintillation vial was charged with **6** (213 mg, 0.189 mmol) and 5 mL of toluene. Solid $CuCl_2$ (27 mg, 0.201 mmol) was added, causing an immediate color change to dark purple. After 4 h, the solution was filtered through a Celite-packed Pasteur pipet. The Celite was then washed with 8 mL of DME. The solution was stripped of volatiles under reduced pressure. The dark purple solid was dissolved in 2 mL of DME and filtered through a Celite-packed Pasteur pipet. Microcrystalline solid for elemental analysis was grown over 14 d by layering this solution with 15 mL of hexanes and storing it at −30 °C (146 mg, 0.150 mmol, 79%). ^{1}H NMR (C_6D_6, 400 MHz, 298 K): δ 8.59 (d, 2H, bpy-*H*), 7.38 (s, 4H, Ar*H*), 7.11 (s, 4H, Ar*H*), 6.84 (t, 2H, bpy-*H*), 6.20 (t, 2H, bpy-*H*), 5.54 (d, 2H, CH_2), 4.00 (d, 2H, CH_2), 2.34 (s, 12H, CH_3), 1.32 (s, 36H, C(CH_3)). Anal. Calcd for $C_{56}H_{68}CeN_2O_4$: C, 69.11; H, 7.04; N, 2.88. Found: C, 68.61; H, 6.9; N, 2.58.

[Li(Ph$_2$CO)Ce(MBP)$_2$(Ph$_2$CO)$_2$] (8). A 20 mL scintillation vial was charged with **1** (243 mg, 0.218 mmol) and 10 mL of toluene. Solid benzophenone (121 mg, 0.664 mmol) was added causing an immediate color change to dark red. After 1 h, the solution was stripped of volatiles under reduced pressure. The red residue was dissolved in 3 mL of toluene and filtered through a Celite-packed Pasteur pipet. Red crystalline solids suitable for X-ray crystallography and elemental analysis were grown over 24 h by layering with 15 mL of hexane (226 mg, 0.165 mmol, 76%). ^{1}H NMR (C_6D_6, 400 MHz, 298 K): δ 15.08 (bs $\Delta\nu_{1/2}$ = 70 Hz), 14.83 (bs $\Delta\nu_{1/2}$ = 150 Hz), 8.82 (bs $\Delta\nu_{1/2}$ = 200 Hz), 7.23 (bs $\Delta\nu_{1/2}$ = 30 Hz), 4.36 (bs $\Delta\nu_{1/2}$ = 40 Hz), −2.84 (s), −4.26 (bs $\Delta\nu_{1/2}$ = 40 Hz), −5.97 (bs $\Delta\nu_{1/2}$ = 1500 Hz), −7.38 (bs $\Delta\nu_{1/2}$ = 30 Hz), −19.56 (bs $\Delta\nu_{1/2}$ = 70 Hz). Definitive ^{1}H NMR peak assignments could not be made due to paramagnetic broadening. ^{7}Li NMR (C_6D_6, 400 MHz, 298 K): δ 4.16 (s). Anal. Calcd for $C_{92}H_{98}CeO_7$: C, 75.90; H, 6.78. Found: C, 75.72; H, 6.46.

■ ASSOCIATED CONTENT

Ⓢ Supporting Information

X-ray crystallographic information in CIF format, table of crystallographic data, and electrochemical data. This material is available free of charge via the Internet at http://pubs.acs.org.

■ AUTHOR INFORMATION

Corresponding Author

*E-mail: schelter@sas.upenn.edu.

Author Contributions

All authors have given approval to the final version of the manuscript.

Notes

The authors declare no competing financial interest.

■ ACKNOWLEDGMENTS

The authors gratefully acknowledge the Chemical Sciences, Geosciences, and Biosciences Division, Office of Basic Energy Sciences, Early Career Research Program of the U.S. Department of Energy, under Award No. DE-SC0006518 for partial support of B.D.M. The University of Pennsylvania is acknowledged for financial support. The University Research Foundation at the University of Pennsylvania is also acknowledged for support of the UV-vis-near-IR spectrophotometer. We thank the National Science Foundation for support of the X-ray diffractometer (Grant CHE-0840438).

■ REFERENCES

(1) Molander, G. A.; Harris, C. R. *Chem. Rev.* **1996**, *96*, 307−338.
(2) Nair, V.; Deepthi, A. *Chem. Rev.* **2007**, *107*, 1862−1891.
(3) Procter, D. J.; Flowers, R. A.; Skrydstrup, T. *Organic Synthesis using Samarium Diiodide*; RSC Publishing: Cambridge, U.K., 2010.
(4) Nair, V.; Balagopal, L.; Rajan, R.; Mathew, J. *Acc. Chem. Res.* **2004**, *37*, 21−30.
(5) Sridharan, V.; Meneñdez, J. C. *Chem. Rev.* **2010**, *110*, 3805−3849.
(6) Nief, F. *Dalton Trans.* **2010**, *39*, 6589−6598.
(7) Hitchcock, P. B.; Lappert, M. F.; Maron, L.; Protchenko, A. V. *Angew. Chem., Int. Ed.* **2008**, *47*, 1488−1491.
(8) MacDonald, M. R.; Bates, J. E.; Fieser, M. E.; Ziller, J. W.; Furche, F.; Evans, W. J. *J. Am. Chem. Soc.* **2012**, *134*, 8420−8423.
(9) Evans, W. J.; Lee, D. S.; Rego, D. B.; Perotti, J. M.; Kozimor, S. A.; Moore, E. K.; Ziller, J. W. *J. Am. Chem. Soc.* **2004**, *126*, 14574−14582.
(10) Morton, C.; Alcock, N. W.; Lees, M. R.; Munslow, I. J.; Sanders, C. J.; Scott, P. *J. Am. Chem. Soc.* **1999**, *121*, 11255−11256.
(11) Dröse, P.; Crozier, A. R.; Lashkari, S.; Gottfriedsen, J.; Blaurock, S.; Hrib, C. G.; Maichle-Mössmer, C. c.; Schädle, C.; Anwander, R.; Edelmann, F. T. *J. Am. Chem. Soc.* **2010**, *132*, 14046−14047.
(12) Hitchcock, P. B.; Hulkes, A. G.; Lappert, M. F. *Inorg. Chem.* **2004**, *43*, 1031−1038.
(13) Arnold, P. L.; Casely, I. J.; Zlatogorsky, S.; Wilson, C. *Helv. Chim. Acta* **2009**, *92*, 2291−2303.
(14) The value of 1.30 V vs Fc/Fc$^+$ was arrived at by subtracting the value for aqueous ferrocene, 0.400 V vs NHE, from the value for the cerium couple, 1.70 V vs NHE. Cerium: Smith, G. F.; Getz, C. A. *Ind. Eng. Chem., Anal. Ed.* **1938**, *10*, 191−195. Aqueous ferrocene: Bond, A. M.; McLennan, E. A.; Stojanovic, R. S.; Thomas, F. G. *Anal. Chem.* **1987**, *59*, 2853−2860.
(15) Butman, L. A.; Sokol, V. I.; Porai-Koshits, M. A. *Koord. Khim.* **1976**, *2*, 265−271.
(16) Streitwieser, A.; Kinsley, S. A.; Jenson, C. H.; Rigsbee, J. T. *Organometallics* **2004**, *23*, 5169−5175.
(17) Sofen, S. R.; Cooper, S. R.; Raymond, K. N. *Inorg. Chem.* **1979**, *18*, 1611−1616.
(18) Bian, Y.; Jiang, J.; Tao, Y.; Choi, M. T. M.; Li, R.; Ng, A. C. H.; Zhu, P.; Pan, N.; Sun, X.; Arnold, D. P.; Zhou, Z.-Y.; Li, H.-W.; Mak, T. C. W.; Ng, D. K. P. *J. Am. Chem. Soc.* **2003**, *125*, 12257−12267.
(19) Robinson, J. R.; Carroll, P. J.; Walsh, P. J.; Schelter, E. J. *Angew. Chem., Int. Ed.* **2012**, 10159−10163.
(20) Bauer, D.; Diamond, D.; Li, J.; McKittrick, M.; Sandalow, D.; Telleen, P. *U.S. Department of Energy Critical Materials Strategy*; U.S. Department of Energy: Washington, DC, 2011; pp 81−84.
(21) Avellaneda, C. O.; Berton, M. A. C.; Bulhões, L. O. S. *Sol. Energy Mater. Sol. Cells* **2008**, *92*, 240−244.
(22) Broderick, E. M.; Thuy-Boun, P. S.; Guo, N.; Vogel, C. S.; Sutter, J. R.; Miller, J. T.; Meyer, K.; Diaconescu, P. L. *Inorg. Chem.* **2011**, *50*, 2870−2877.
(23) Li, T.; Li, F.; Lü, J.; Guo, Z.; Gao, S.; Cao, R. *Inorg. Chem.* **2008**, *47*, 5612−5615.
(24) Wester, D. W.; Palenik, G. J.; Palenik, R. C. *Inorg. Chem.* **1985**, *24*, 4435−4437.
(25) Yu, P.; O'Keefe, T. J. *J. Electrochem. Soc.* **2006**, *153*, C80−C85.
(26) Gottfriedsen, J. *Z. Anorg. Allg. Chem.* **2005**, *631*, 2928−2930.
(27) Stilinović, V.; Kaitner, B. *J. Coord. Chem.* **2009**, *62*, 2698−2708.
(28) Aspinall, H. C.; Bacsa, J.; Jones, A. C.; Wrench, J. S.; Black, K.; Chalker, P. R.; King, P. J.; Marshall, P.; Werner, M.; Davies, H. O.; Odedra, R. *Inorg. Chem.* **2011**, *50*, 11644−11652.
(29) Deng, M.; Yao, Y.; Shen, Q.; Zhang, Y.; Sun, J. *Dalton Trans.* **2004**, 944−950.
(30) Qi, R.; Liu, B.; Xu, X.; Yang, Z.; Yao, Y.; Zhang, Y.; Shen, Q. *Dalton Trans.* **2008**, 5016−5024.
(31) Xu, X.; Ma, M.; Yao, Y.; Zhang, Y.; Shen, Q. *Eur. J. Inorg. Chem.* **2005**, *2005*, 676−684.
(32) Xu, X.; Zhang, Z.; Yao, Y.; Zhang, Y.; Shen, Q. *Inorg. Chem.* **2007**, *46*, 9379−9388.

(33) Yao, Y.; Xu, X.; Liu, B.; Zhang, Y.; Shen, Q.; Wong, W.-T. *Inorg. Chem.* **2005**, *44*, 5133−5140.
(34) Liang, Z.; Ni, X.; Li, X.; Shen, Z. *Inorg. Chem. Commun.* **2011**, *14*, 1948−1951.
(35) Shannon, R. *Acta Crystallogr., Sect. A: Found. Crystallogr.* **1976**, *32*, 751−767.
(36) Connelly, N. G.; Geiger, W. E. *Chem. Rev.* **1996**, *96*, 877−910.
(37) Morss, L. R. *Chem. Rev.* **1976**, *76*, 827−841.
(38) Moore, J. A.; Cowley, A. H.; Gordon, J. C. *Organometallics* **2006**, *25*, 5207−5209.
(39) Vasudevan, K.; Cowley, A. H. *Chem. Commun.* **2007**, 3464−3466.
(40) Bartecki, A.; Burgess, J. *The Colour of Metal Compounds*; Gordon and Breach Science Publishers: Amsterdam, 2000; p 127.
(41) Vogler, A.; Kunkely, H. *Inorg. Chim. Acta* **2006**, *359*, 4130−4138.
(42) Mandel, G.; Bauman, R. P.; Banks, E. *J. Chem. Phys.* **1960**, *33*, 192−193.
(43) Booth, C. H.; Walter, M. D.; Kazhdan, D.; Hu, Y.-J.; Lukens, W. W.; Bauer, E. D.; Maron, L.; Eisenstein, O.; Andersen, R. A. *J. Am. Chem. Soc.* **2009**, *131*, 6480−6491.
(44) Mohammad, A.; Cladis, D. P.; Forrest, W. P.; Fanwick, P. E.; Bart, S. C. *Chem. Commun.* **2012**, *48*, 1671−1673.
(45) Veauthier, J. M.; Schelter, E. J.; Carlson, C. N.; Scott, B. L.; Re, R. E. D.; Thompson, J. D.; Kiplinger, J. L.; Morris, D. E.; John, K. D. *Inorg. Chem.* **2008**, *47*, 5841−5849.
(46) Fukuzumi, S.; Satoh, N.; Okamoto, T.; Yasui, K.; Suenobu, T.; Seko, Y.; Fujitsuka, M.; Ito, O. *J. Am. Chem. Soc.* **2001**, *123*, 7756−7766.
(47) In the noncoordinating solvent fluorobenzene, very irreversible electrochemistry in both the presence and absence of bipyridine has, as of yet, prevented a meaningful analysis.
(48) Evans, W. J.; Drummond, D. K. *J. Am. Chem. Soc.* **1989**, *111*, 3329−3335.
(49) Al-Karaghouli, A. R.; Wood, J. S. *Inorg. Chem.* **1972**, *11*, 2293−2299.
(50) Gulino, A.; Casarin, M.; Conticello, V. P.; Gaudiello, J. G.; Mauermann, H.; Fragala, I.; Marks, T. J. *Organometallics* **1988**, *7*, 2360−2364.
(51) Bewick, A.; Jones, V. W.; Kalaji, M. *Electrochim. Acta* **1996**, *41*, 1961−1970.
(52) Fleischer, E. B.; Sung, N.; Hawkinson, S. *J. Phys. Chem.* **1968**, *72*, 4311−4312.
(53) Clegg, W.; Izod, K.; O'Shaughnessy, P.; Eaborn, C.; Smith, J. D. *Angew. Chem., Int. Ed. Engl.* **1997**, *36*, 2815−2817.
(54) Thomson, R. K.; Scott, B. L.; Morris, D. E.; Kiplinger, J. L. *C. R. Chim.* **2010**, *13*, 790−802.
(55) Bruker *SAINT*; Bruker AXS Inc.: Madison, Wisconsin, USA, 2009.
(56) Bruker *SHELXTL*; Bruker AXS Inc.: Madison, Wisconsin, USA, 2009.
(57) Sheldrick, G. M. *TWINABS*. University of Gottingen: Gottingen, Germany, 2008.
(58) Sheldrick, G. M. *SADABS*. University of Gottingen: Gottingen, Germany, 2007.
(59) Sheldrick, G. M. *Acta Crystallogr.* **2008**, *A64*, 112−122.
(60) Spek, A. L. *PLATON, A Multipurpose Crystallographic Tool*; Utrecht University: Utrecht, Netherlands, 2005.